Cathepsin D and Eukaryotic Translation Elongation Factor 1 as Promising Markers of Cellular Senescence

Hae-Ok Byun,[1] Na-Kyung Han,[1,4] Hae-June Lee,[2] Ki-Bum Kim,[4] Young-Gyu Ko,[4] Gyesoon Yoon,[5] Yun-Sil Lee,[2] Seok-Il Hong,[3] and Jae-Seon Lee[1]

Divisions of [1]Radiation Cancer Research and [2]Radiation Effects, and [3]Department of Laboratory Medicine and Clinical Pathology, Korea Institute of Radiological and Medical Sciences; [4]Graduate School of Life Sciences and Biotechnology, Korea University, Seoul, Korea and [5]Department of Biochemistry, School of Medicine, and Department of Molecular Science and Technology, Graduate School, Ajou University, Suwon, Korea

Abstract

Induction of premature senescence may be a promising strategy for cancer treatment. However, biomarkers for senescent cancer cells are lacking. To identify such biomarkers, we performed comparative proteomic analysis of MCF7 human breast cancer cells undergoing cellular senescence in response to ionizing radiation (IR). IR-induced senescence was associated with up-regulation of cathepsin D (CD) and down-regulation of eukaryotic translation elongation factor 1β2 (eEF1B2), as confirmed by Western blot. The other elongation factor, eukaryotic translation elongation factor 1α1 (eEF1A1), was also down-regulated. IR-induced senescence was associated with similar changes of CD and eEF1 (eEF1A1 and eEF1B2) levels in the HCT116 colon cancer cell line and the H460 lung cancer cell line. Up-regulation of CD and down-regulation of eEF1 seemed to be specific to senescence, as they were observed during cellular senescence induced by hydrogen peroxide or anticancer drugs (camptothecin, etoposide, or 50 ng doxorubicin) but not during apoptosis induced by Taxol or 10 μg doxorubicin or autophagy induced by tamoxifen. The same alterations in CD and eEF1A1 levels were observed during replicative senescence and Ras oncogene-induced senescence. Transient cell cycle arrest did not alter levels of eEF1 or CD. Chemical inhibition of CD (pepstatin A) and small interfering RNA–mediated knockdown of CD and eEF1 revealed that these factors participate in cell proliferation. Finally, the senescence-associated alteration in CD and eEF1 levels observed in cell lines was also observed in IR-exposed xenografted tumors. These findings show that CD and eEF1 are promising markers for the detection of cellular senescence induced by a variety of treatments. [Cancer Res 2009;69(11):4638–47]

Introduction

Cellular senescence was originally described in normal human cells undergoing a finite number of divisions before permanent growth arrest (1). Cells undergoing such replicative senescence are metabolically active and exhibit distinct morphologic changes and phenotypic markers (2). Cellular senescence has recently become regarded as a general biological program of terminal growth arrest because a variety of treatments have been shown to trigger cellular senescence. The activated *ras* or *raf* oncogenes trigger senescence in normal cells, and low doses of DNA-damaging agents, including ionizing radiation (IR) and chemotherapeutic drugs, induce senescent phenotypes in cancer cells (3–6). Accumulating evidences suggest that apoptosis may not be the exclusive or even the primary mechanism underlying loss of self-renewal capacity in IR- or drug-treated cancer cells (5–7). Recent studies suggest that induction of premature senescence is a promising treatment for solid tumors (8, 9).

The characteristic phenotypes of premature senescence are abundant in premalignant neoplastic lesions (10). Premature senescence is not only a barrier to tumorigenesis but also a hallmark of premalignant tumors (10, 11). Therefore, senescence markers could be useful diagnostic and prognostic tools (12). The most commonly used senescence biomarker is senescence-associated β-galactosidase (SA-β-Gal; ref. 2). Senescence-associated heterochromatic foci are also considered senescence markers (12). However, these markers have the disadvantage of being unable to be detected using standard immunohistochemical methods. Recently, DNA microarray analysis identified the oncogene-induced premature senescence markers p15INK4b, DCR2, and DEC1 (10). However, senescence markers in action are still a few. Therefore, additional specific markers of premature senescence that have diagnostic and prognostic value await identification.

Radiotherapy and chemotherapy, major regimens of cancer treatment, recently have been proved to induce premature senescence (5–7). The aim of this study was to identify and validate useful biomarkers for the detection of cellular senescence using comparative proteomic analysis. Here, we provide evidence that eukaryotic elongation factor 1 (eEF1) and cathepsin D (CD) are reliable markers of cellular senescence.

Materials and Methods

Materials. Pepstatin A, doxorubicin, tamoxifen, and camptothecin were purchased from Calbiochem. eEF1A1 and eukaryotic translation elongation factor 1β2 (eEF1B2) antibodies were purchased from Abcam. Phospho-pRb antibody was purchased from Cell Signaling Technology, and LC3 antibody and Taxol (paclitaxel) were obtained from Sigma. Cyclin-dependent kinase (CDK) 2, CDK4, cyclin B, cyclin D, β-actin, CD, p53, and p21 antibodies were obtained from Santa Cruz Biotechnology. DMEM, RPMI 1640, McCoy's 5A medium, and fetal bovine serum (FBS) were from WelGENE.

Cell culture and irradiation. MCF7, MDA-MB231, normal human fibroblasts (NHF), and human embryonic fibroblast (HEF) were cultured in DMEM; H460 cells were cultured in RPMI 1640; and HCT116 cells were cultured in McCoy's 5A medium supplemented with 10% FBS and 1% penicillin and streptomycin solution at 37°C in a 5% CO_2 incubator. Young (PD 34) and old (PD 62) NHF was kindly supplied by Prof. E.S. Hwang (University of Seoul, Seoul, Korea), and HEF was generously supplied by Prof. J-Y. Lee (Hallym University, Chuncheon, Korea).

Note: Supplementary data for this article are available at Cancer Research Online (http://cancerres.aacrjournals.org/).

Requests for reprints: Jae-Seon Lee, Division of Radiation Cancer Research, Korea Institute of Radiological and Medical Sciences, Seoul 139-706, Korea. Phone: 82-2-970-1388; Fax: 82-2-970-1388; E-mail: jaeslee@kcch.re.kr.

doi:10.1158/0008-5472.CAN-08-4042

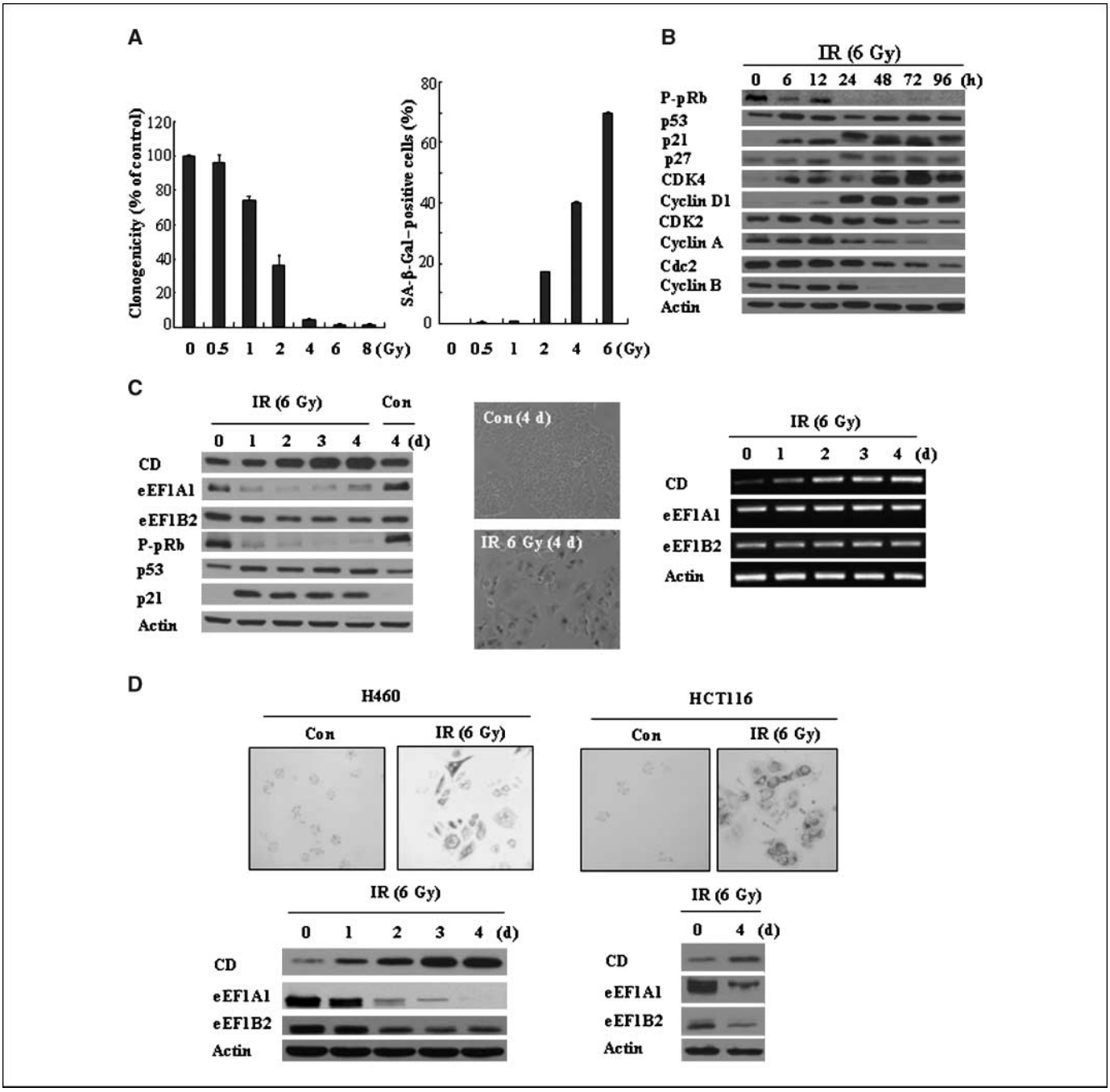

Figure 1. Differential levels of CD and eEF1 during IR-induced senescence. *A,* dose-dependent induction of cellular senescence in IR-exposed MCF7 cells. *Left,* clonogenic survival; *right,* SA-β-Gal activity. *B,* Western blot analysis of cell cycle regulatory proteins in 6 Gy IR-exposed MCF7 cells. *C,* levels of CD and eEF1, SA-β-Gal staining, and RT-PCR analysis in IR-induced senescent MCF7 cells. Cells maintained for 4 d in the absence of IR exposure served as controls. *D,* SA-β-Gal staining and Western blot analyses of senescent H460 (*left*) and HCT116 cells (*right*) exposed to 6 Gy IR.

For irradiation, cells were exposed to γ-ray with a ^{137}Cs γ-ray source (Atomic Energy of Canada Ltd.) at a dose rate of 3.2 Gy/min.

Production of recombinant retrovirus. MFGPuro H-ras^{V12} or MFGPuro retroviral vectors were generously provided by Prof. S-J. Lee (Hanyang University, Seoul, Korea). Preparation of viral supernatant was performed as described by Choi and colleagues (13).

Two-dimensional electrophoresis and identification of protein spots. Two-dimensional gel electrophoresis (2-DE) and electrospray ionization-tandem mass spectrometry (ESI-MS/MS) were performed as described by Kim and colleagues (14).

Cell growth rate and colony-forming assay. Cell growth rate was monitored by counting cells with a hemocytometer. Clonogenicity was examined by colony-forming assay. Colonies grown for 10 to 12 d were stained with Diff-Quick (Sysmex Corp.) and counted using Artek Counter (Imaging Products International, Inc.).

Senescence-associated β-galactosidase staining. Cells or tissues were stained for β-galactosidase activity as described by Dimri and colleagues (2).

Reverse transcription-PCR. Total RNA was prepared using Trizol reagent (Invitrogen) and used as a template for cDNA synthesis with Moloney murine leukemia virus reverse transcriptase using SuperScript III

reverse transcriptase kits (Invitrogen). The primer sequences were as follows: CD, 5′-AAAGGCCCCGTCTCAAAGTA-3′ (forward) and 5′-CAAGCGATGTCCAGCAGTTT-3′ (reverse); eEF1B2, 5′-CAAATATGGTCCTGCCGATG-3′ (forward) and 5′-GATGAGCCCCAGACTAAGCC-3′ (reverse); and eEF1A1, 5′-TGAACCATCCAGGCCAAATA-3′ (forward) and 5′-ATCACGAACAGCAAAGCGAC-3′ (reverse).

Small interfering RNA. Small interfering RNAs (siRNA) of eEF1A1 and CD were obtained from Santa Cruz Biotechnology. siRNA of eEF1B2 was purchased from Ambion, Inc. Transfection was performed with RNAiMAX (Invitrogen).

Western blotting. Western blot analysis was conducted as described by Lee and colleagues (15).

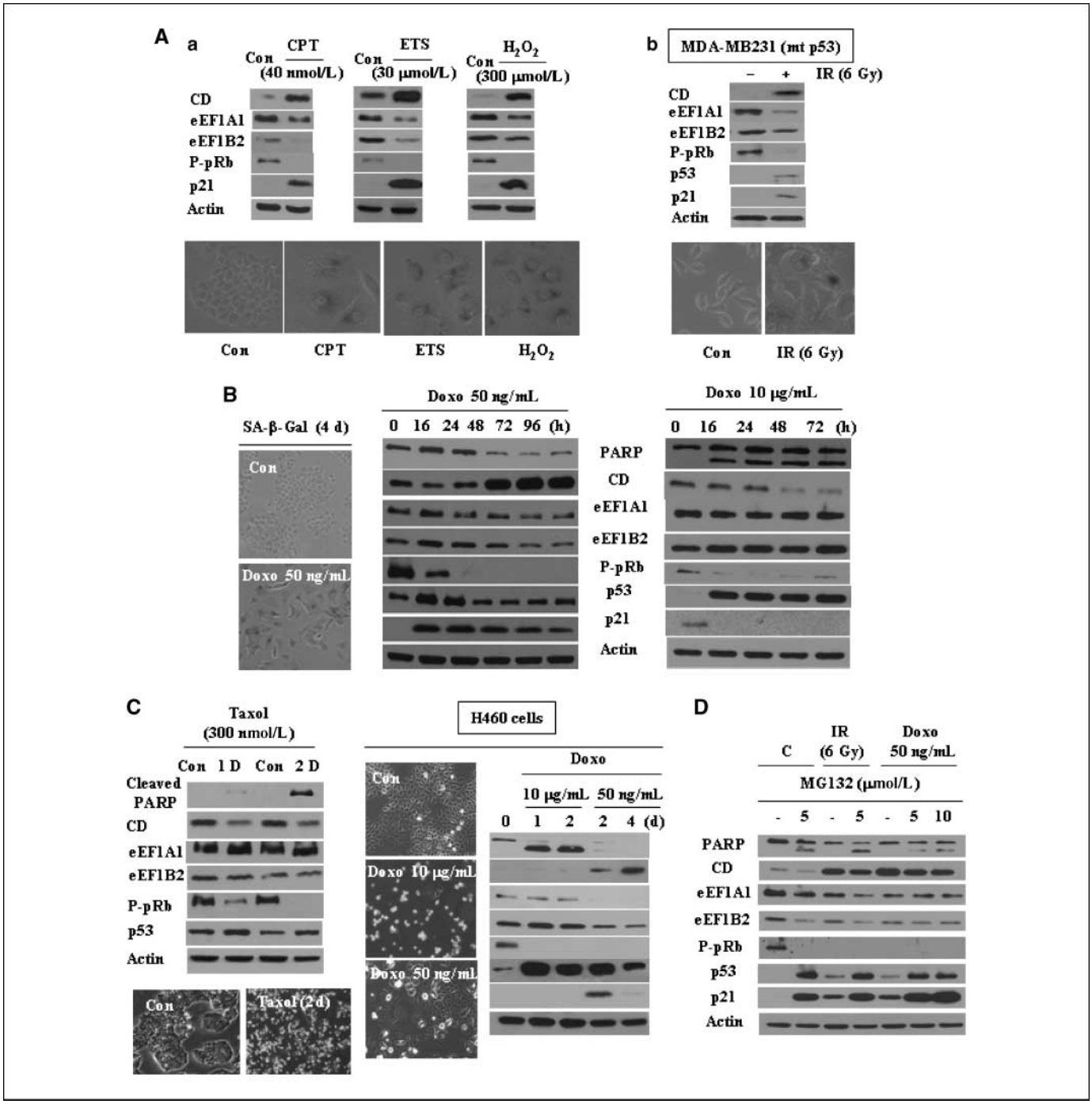

Figure 2. Comparison of CD and eEF1 levels between senescence and apoptosis. *A, a,* Western blot and SA-β-Gal activity of MCF7 cells undergoing treatment-induced senescence in response to a 4-d treatment with 40 nmol/L camptothecin (*CPT*), 30 μmol/L etoposide (*ETS*), or 300 μmol/L hydrogen peroxide (H_2O_2). *b,* Western blot and SA-β-Gal activity of MDA-MB231 p53 mutant cells exposed to 6 Gy IR. *B,* SA-β-Gal staining and protein levels in doxorubicin-induced senescence (low dose, 50 ng/mL) or apoptosis (high dose, 10 μg/mL) of MCF7 cells. PARP cleavage served as an apoptotic marker. *C,* CD and eEF levels in Taxol (300 nmol/L)–treated apoptotic MCF7 cells (*left*) and in H460 cells undergoing doxorubicin-induced senescence (10 μg/mL doxorubicin) or apoptosis (50 ng/mL doxorubicin; *right*). *D,* effect of MG132 on IR- or doxorubicin-induced changes in eEF1 and CD levels. Cells were cultured for 72 h after treatment with IR or doxorubicin (low dose, 50 ng/mL) and then treated with MG132 for 16 h.

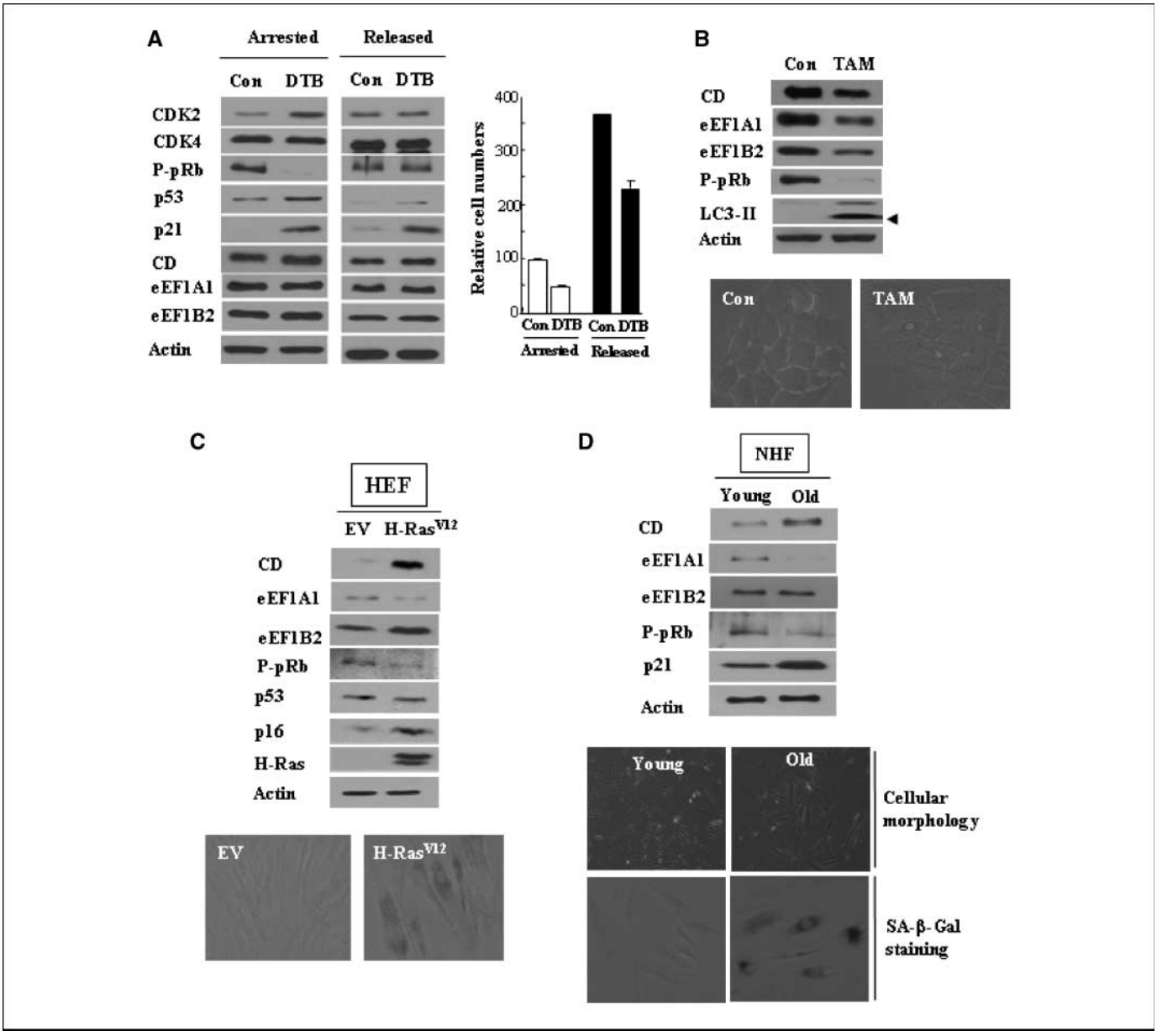

Figure 3. Protein levels of CD and eEF1 in transient cell cycle arrest, autophagy, oncogene-induced senescence, and replicative senescence. *A,* effect of transient cell cycle arrest on CD and eEF1 protein levels. MCF7 cells were synchronized by DTB treatment (15 h, 0.5 mg/mL; *Arrested*) and incubated for an additional 48 h without DTB (*Released*). Control cells were maintained in an identical manner except that they were kept in medium containing thymidine. *B,* CD and eEF1 levels in MCF7 cells underwent autophagy by the treatment of tamoxifen (10 μmol/L) for 2 d. *C,* CD and eEF1 levels in oncogenic Ras-induced senescence. HEFs were infected with virus containing empty vector (*EV*) or H-ras^{V12} retroviral vector and were incubated for 8 d. *D,* CD and eEF1 levels in young (PD 34) and old (PD 62) NHFs.

Measurement of CD activity. CD proteolytic activity was analyzed using a fluorogenic CD activity kit from Sigma.

Animals. All animal protocols and studies were conducted in accordance with the guidelines of the Institutional Animal Care and Use Committee in Korea Institute of Radiological and Medical Sciences. Six-week-old BALB/c athymic nude mice were obtained from Japan SLC, Inc. All animals were placed at an animal care facility, maintained at controlled temperature (22 ± 1%) and humidity (50 ± 5%) under regular 14-h light/10-h dark cycle. Pellet diets (Cargill Agri Purina, Inc.) and water were supplied *ad libitum*.

Establishment of xenograft tumor. A single-cell suspension of H460 cells (1×10^7) was injected s.c. into bilateral hind legs of BALB/c nude mice ($n = 6$). When the tumor reached a volume of 150 to 200 mm^3, tumor on the left hind leg was irradiated with total dose of 12 Gy in three fractions (4 Gy once every 3 d), and tumor on the right side was unirradiated as control. Local regional irradiation of tumors was done under anesthesia using a ^{60}Co source irradiator (Theratron 780, Atomic Energy of Canada) operating at 1.3 Gy/min. At 8 d after completion of irradiation, animals were sacrificed and tumors were harvested. Tumor volumes were determined according to the formula $(L \times W^2)/2$ by measuring tumor length (L) and width (W) with a caliper.

Immunohistochemical analysis. For detection of cell proliferation and apoptosis, immunohistochemistry was performed as described by Lee and colleagues (15).

Statistics. Statistical values were expressed as mean ± SE. Statistical analysis was performed using the Student's t test. Significance levels were set at $P < 0.05$.

Results

IR induces cellular senescence in MCF7 cells. To determine the efficiency with which IR induces cellular senescence in cancer

cells, we analyzed clonogenicity and SA-β-Gal activity in MCF7 human breast cancer cells exposed to various doses of IR (Fig. 1*A*). An IR dose of 6 Gy effectively arrested cell proliferation and induced cellular senescence. Over 4 days after irradiation, cells exhibited a progressive increase in senescence-specific morphology, as seen by a large, flat cellular shape and SA-β-Gal activity (Fig. 1*A*; Supplementary Fig. S1). Western blot analysis revealed p53 activation, p21 induction, and loss of phospho-pRb at an early stage of senescence (Fig. 1*B*). The cell cycle regulators CDK2, Cdc2, cyclin A, and cyclin B were gradually decreased, whereas CDK4 and cyclin D were gradually increased. In all cases, these changes were sustained for up to 4 days. Increased p21 could bind to

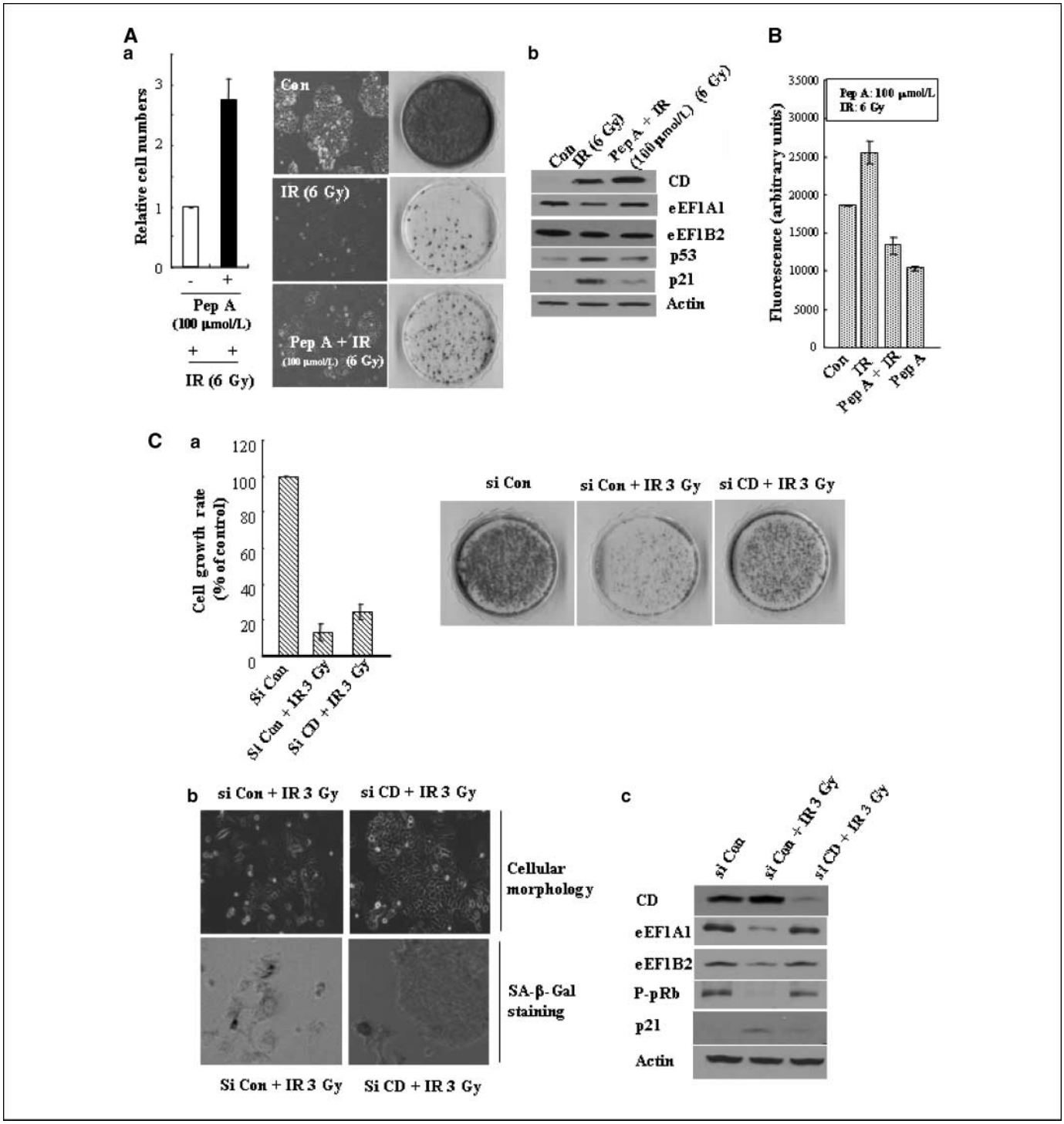

Figure 4. Effect of CD inhibition on cell proliferation. *A,* effect of pepstatin A (*Pep A*) on cell growth and colony-forming ability (*a*), and CD and eEF1 levels (*b*) of MCF7 cells exposed to 6 Gy IR. Cells were analyzed at 5 or 12 d (for colony-forming assay) after treatment. *B,* CD proteolytic activities at 24 h after treatment in MCF7 cells. *C,* effect of siRNA-mediated CD knockdown on cell growth and colony-forming ability (*a*), SA-β-Gal staining (*b*), and protein level (*c*). MCF7 cells were transfected with 100 nmol/L CD siRNA and analyzed 6 or 9 d (for colony-forming assay) later.

cyclin D1-CDK4 complex and proliferating cell nuclear antigen, and resulted in G_1 arrest (16, 17). Consistent with these results, IR-treated cells underwent G_1 arrest (data not shown), and treatment-induced senescence was almost complete at 4 days after irradiation.

Proteins undergoing level changes during IR-induced senescence of MCF7 cells. To identify proteins undergoing level changes during IR-induced senescence, comparative proteomic analysis was performed in control cells and cells exhibiting senescent phenotypes following exposure to 6 Gy IR. A representative 2-DE pattern is shown in Supplementary Fig. S2. Two protein spots were reproducibly up-regulated or down-regulated during IR-induced senescence. ESI-MS/MS analysis identified these factors as chain B of CD and eEF1B2 (Supplementary Table S1).

Altered protein levels of CD and eEF1 during IR-induced or chemotherapeutic drug–induced senescence. Western blot and reverse transcription-PCR (RT-PCR) analyses were performed to confirm that CD and eEF1B2 undergo expression changes in IR-induced senescence. CD was up-regulated at the transcriptional level, whereas eEF1B2 was down-regulated at the posttranscriptional level (Fig. 1*C*). Eukaryotic translation elongation factor 1α1 (eEF1A1), other entity of elongation factors, was also down-regulated at the posttranscriptional level. MCF7 control cells that were incubated for 4 days without IR exposure were not positive for SA-β-Gal. Moreover, they did not exhibit any alterations in cellular morphology and in levels of CD or eEF1 (eEF1A1 and eEF1B2) or sustained changes in levels of p53, p21, or phospho-pRb that were indicative of prolonged cell cycle arrest (Fig. 1*C*). Differential levels of CD and eEF1 were also confirmed in the H460 lung cancer cell line and the HCT116 colon cancer cell line (Fig. 1*D*). In both cell lines, CD protein was increased, whereas eEF1 proteins were decreased. Next, we examined CD and eEF1 level changes in response to other senescence-inducing chemotherapeutic drugs (i.e., camptothecin and etoposide) and hydrogen peroxide (18–20). These agents induced alterations in CD and eEF1 levels that were consistent with those seen in IR-treated cells (Fig. 2*A, a*). To determine whether CD and eEF1 alterations were p53 dependent, we analyzed CD and eEF1 levels in IR (6 Gy)–exposed MDA-MB231 cells, which contain mutant p53 (21). These cells yielded consistent results with cells expressing wild-type p53 (Fig. 2*A, b*).

CD up-regulation and eEF1 down-regulation are specific to senescence, not apoptosis. Low doses of chemotherapeutic drug, doxorubicin, induce cellular senescence in carcinoma cells (22, 23). In contrast, high doses of this drug induce apoptosis (23). We determined whether changes in CD and eEF1 protein levels differ according to cell fate (i.e., senescence or apoptosis). At a low dose (50 ng/mL), doxorubicin induced senescence-specific morphologic changes and positive SA-β-Gal staining (Fig. 2*B*; Supplementary Fig. S3). In these cells, decrease of phospho-pRb and accumulation of p21 were accompanied by up-regulation of CD and down-regulation of eEF1 (Fig. 2*B*). In contrast, a high dose of doxorubicin (10 μg/mL) induced apoptosis-specific morphologic changes and poly(ADP-ribose) polymerase (PARP) cleavage (apoptotic marker; Fig. 2*B*; Supplementary Fig. S3). Under these apoptotic conditions, p21 was decreased due to caspase activation as already known. Protein level of eEF1 remained unaltered, whereas CD was gradually decreased. All these changes also occurred in cells undergoing apoptosis in response to Taxol (paclitaxel; Fig. 2*C, left*). Thus, CD and eEF1 are differentially regulated by senescence- or apoptosis-specific signaling pathways. The distinct differences in eEF1 and CD protein levels between apoptosis and senescence were confirmed in H460 cells (Fig. 2*C, right*). To determine if the decreases in PARP and eEF1 associated with IR- or doxorubicin-induced senescence are due to proteasomal degradation, we treated MCF7 cells with the proteasomal inhibitor MG132 (Fig. 2*D*). The results indicate that the proteasomal degradation pathway does not contribute to decrease in PARP or eEF1.

Transient cell cycle arrest and autophagy do not induce CD up-regulation and eEF1 down-regulation. Next, we investigated the effect of transient cell cycle arrest on CD and eEF1 levels. Transient arrest at G_1-S phase was induced by double thymidine block (DTB; ref. 24). G_1-S phase transition arrest was evidenced by a decrease in phospho-pRb and an accumulation in CDK2. DTB led to an accumulation of p53 and p21. No significant alterations in levels of CD and eEF1 were detected at arrested and released conditions (Fig. 3*A, left*). The transience of cell cycle arrest was confirmed by the counting of cell number (Fig. 3*A, right*).

Recently, autophagy has been reported to occur in several types of cancer cells in response to radiation or chemotherapy (25). Because autophagy could lead to growth arrest, a reduction in cell number, and nonapoptotic death, we examined CD and eEF1 protein levels in cells undergoing tamoxifen-induced autophagy (26). Autophagy was confirmed using the autophagy marker LC3-II (Fig. 3*B*; ref. 27). Both CD and eEF1 were decreased under these conditions (Fig. 3*B*), showing that senescence can be distinguished from autophagy and apoptosis based on CD and eEF1 protein levels.

To determine whether CD and eEF1 are relevant markers for replicative or oncogene-induced senescence, we examined levels of these proteins in young and old NHFs or H-ras^{V12}–transfected HEFs. CD was increased and eEF1A1 was decreased during both types of senescence (Fig. 3*C* and *D*). However, eEF1B2 was increased in oncogene-induced senescence and unchanged in replicative senescence (Fig. 3*C* and *D*). This indicates that eEF1A1 and eEF1B2 respond differently to senescence signals. These findings show that CD and eEF1A1 are relevant markers for detecting a variety of types of cellular senescence and that both markers are sufficient to distinguish senescence from other cellular fates.

CD and eEF1 play critical roles in cell proliferation. To understand whether changes in CD and eEF1 protein levels occur as a result of senescence or contribute to this process, we analyzed MCF7 growth in the presence of pepstatin A or siRNAs for CD or eEF1. Pepstatin A is a specific inhibitor of aspartic proteases, such as pepsin, rennin, and CD. However, because CD is the major intracellular aspartic protease, the intracellular effects of pepstatin A could be attributed to inhibition of CD activity (28). We found that cell proliferation was greater in cells exposed to IR in the presence of 100 μmol/L pepstatin A than in their non–pepstatin A-treated counterparts (Fig. 4*A, a*). Effect of pepstatin A on protein levels was assessed (Fig. 4*A, b*). The densitometric quantification of three independent Western blots revealed that eEF1A1 and p21 levels were significantly restored in the presence of pepstatin A ($P < 0.05$). However, pepstatin A did not significantly restore eEF1B2 levels ($P > 0.05$). Because CD level was rather increased by pepstatin A treatment (Fig. 4*A, b*), we measured CD activity using a fluorogenic CD activity kit. We found that CD activity was decreased (Fig. 4*B*). It indicates that CD protein level was not correlated with CD activity in pepstatin A-treated cells. Treatment with pepstatin A alone did not alter levels of eEF1A1, eEF1B2, p21, or p53 (Supplementary Fig. S4*A*). Whereas CD protein level was a little increased (Supplementary Fig. S4*A*), CD activity was inhibited by pepstatin A treatment, as observed in treatment of IR and

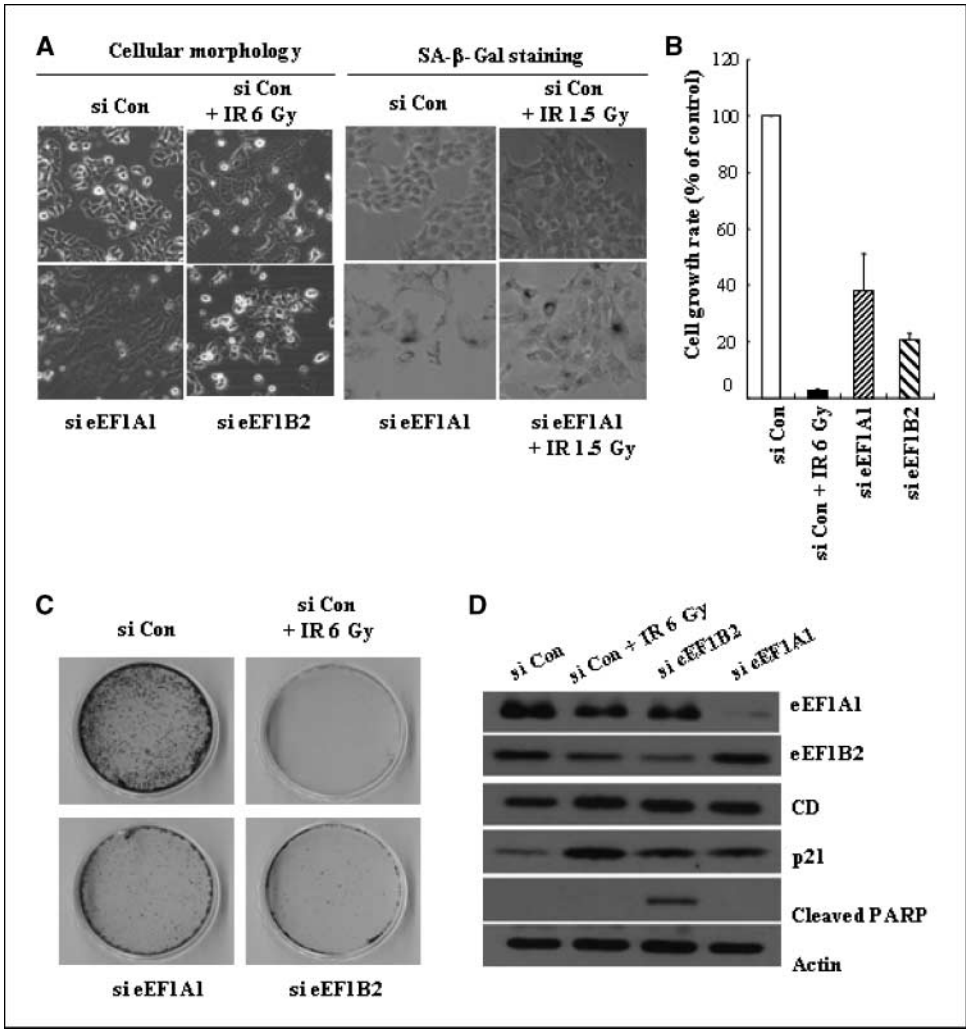

Figure 5. Effect of siRNA-mediated eEF1 knockdown on cell proliferation. *A,* cellular morphology or SA-β-Gal staining of MCF7 cells transfected with 100 nmol/L control siRNA, eEF1A1 siRNA, or eEF1B2 siRNA at 6 d. *B,* relative growth rate. *C,* colony-forming ability at 9 d after transfection. *D,* Western blot analysis of si eEF1A1–expressing or si eEF1B2–expressing MCF7 cells at 6 d after transfection.

pepstatin A (Fig. 4*B*). Cell number was affected by the treatment of pepstatin A alone (Supplementary Fig. S4*B*), indicating that cell growth rate was regulated by CD activity.

Next, we investigated the effect of siRNA-mediated CD knockdown on cell growth and SA-β-Gal activity. The growth rate and colony-forming ability of 3 Gy IR-exposed cells were increased in the presence of CD siRNA than in the presence of control siRNA (Fig. 4*C, a*). CD siRNA decreased SA-β-Gal activity (Fig. 4*C, b*). Western blot analysis revealed that CD siRNA also blocked IR-induced changes in eEF1, phospho-pRb, and p21 levels (Fig. 4*C, c*). These results, taken with results from the pepstatin A experiments, suggest that CD is a pivotal participant in senescence.

Cells transfected with eEF1A1 siRNA had a flattened, large appearance and exhibited SA-β-Gal activity (Fig. 5*A*). Proliferation of these cells was clearly decreased, and in contrast to control siRNA–transfected cells, these cells had barely detectable colony-forming ability (Fig. 5*B* and *C*). On the other hand, eEF1B2 siRNA–transfected cells seemed shrunken, a characteristic not associated with senescence (Fig. 5*A*). Cell number and colony-forming ability were also decreased, and cleaved PARP was present (Fig. 5*B–D*). Knockdown of eEF1 expression in siRNA-transfected cells was confirmed (Fig. 5*D*).

CD and eEF1 as markers of IR-induced senescence in xenografted tumors. Finally, we explored the *in vivo* utility of CD and eEF1 as biomarkers of senescence. BALB/c nude mice were bilaterally xenografted tumors on hind legs ($n = 6$). Control tumors on right hind legs were left unirradiated, whereas tumors on left hind legs were irradiated with a 12 Gy dose of γ-rays, administered in three fractions (4 Gy once every 3 days). Eight days after the final irradiation, tumor volumes were measured (Fig. 6*A*), and the CD and eEF1 levels were analyzed (Fig. 6*B*). In all mice, irradiated tumors exhibited CD up-regulation, with the average fold change being 2.48 ± 0.78 (mean ± SE). Fifty percent of mice showed a notable change in eEF1A1 and eEF1B2 (>30% decrease compared with control), with the average fold change being 0.36 ± 0.08 and 0.53 ± 0.03, respectively. Immunohistologic assays revealed that the rate of apoptosis was similar between control and IR-exposed tumor tissue (Fig. 6*C*). However, cell proliferation, which was detected with the cell proliferation marker Ki-67, was evident only in control tumor tissue. Conversely, only IR-exposed tumor tissue contained SA-β-Gal–positive cells. This finding, taken with the changes observed in CD and eEF1 protein levels, suggests that IR-induced senescence was contributed to the low proliferation rate in this tissue.

Discussion

The fate of irradiated cells is controlled by a network of signaling molecules and can range from premature senescence to mitotic

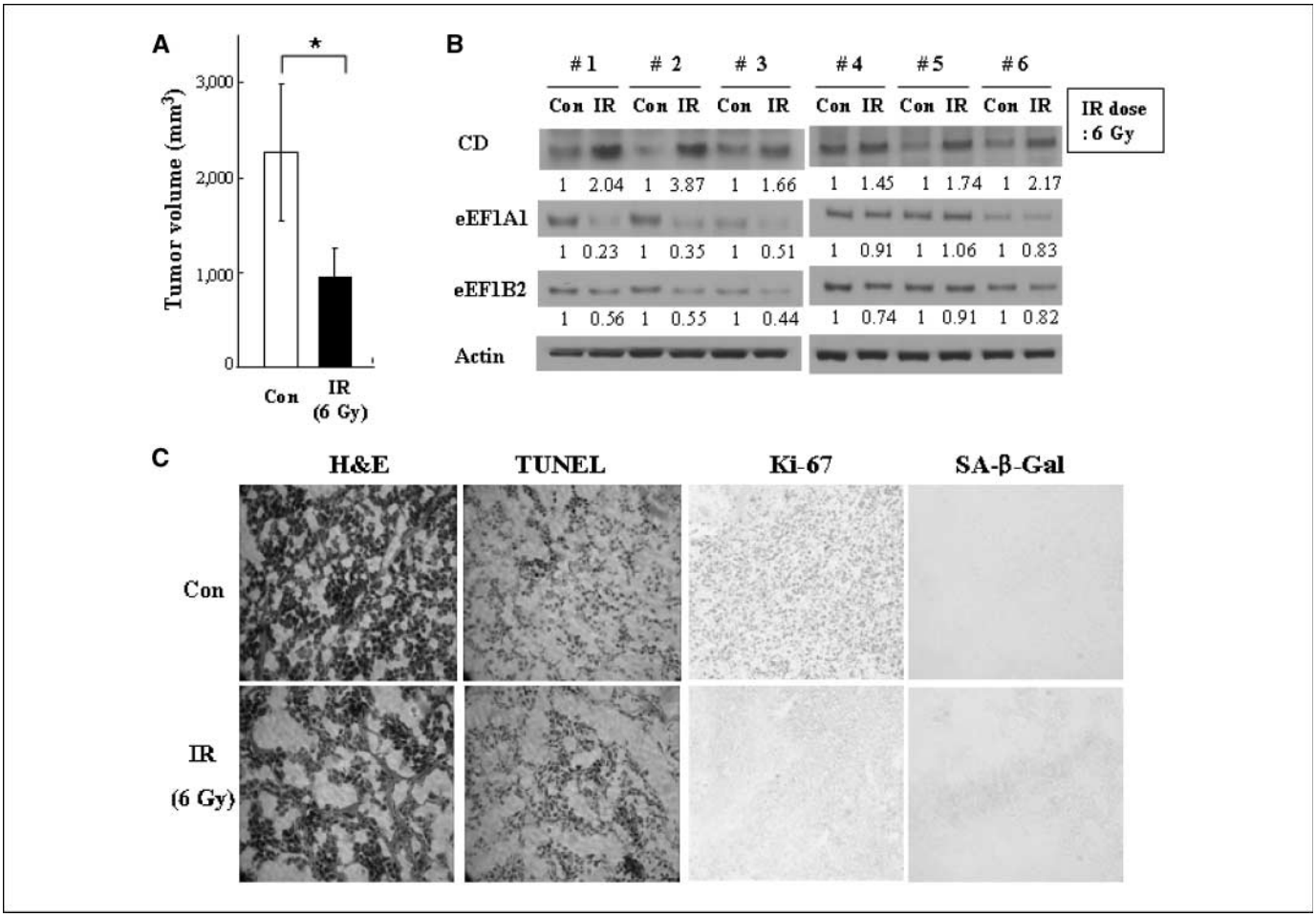

Figure 6. Levels of eEF1 and CD in xenografted tumors. *A,* tumor volume. *Columns,* mean ($n = 6$); *bars,* SE. *, $P < 0.01$. *B,* Western blot analysis of tumor tissues. Protein levels were measured by scanning densitometry and normalized to levels of the loading control (actin). Values below the blots indicate protein levels relative to the control. *C,* tumor tissue analysis by H&E staining, Ki-67 immunohistochemistry (cell proliferation detection), terminal deoxynucleotidyl transferase–mediated dUTP nick end labeling (*TUNEL*; apoptosis detection), and SA-β-Gal staining (senescence detection).

catastrophe or apoptosis. The extent to which apoptosis and other types of cell death contribute to radiation treatment-induced death is an ongoing controversy (29). Some evidence suggests that senescence, not apoptosis, determines long-term responses to tumor treatment, with this response depending on the cellular status (30). Indeed, senescence induction is increased to compensate for inactivation of the apoptotic program (31). If the senescence program remains intact when oncogenes promote aberrant cell proliferation, the neoplastic lesion may stay in a premalignant state (10). Cellular senescence, like apoptosis, plays an important role in anticancer defense *in vivo* (32–34). Recent *in vivo* studies provide evidence that senescence participates in tumor suppression. For example, cellular senescence is crucial in restricting tumorigenesis in Pten-deficient prostate and in lymphomagenesis (35, 36). In $Terc^{-/-}$ mice, cellular senescence suppresses spontaneous tumorigenesis in the presence of a functional p53 signaling pathway (37). Moreover, tumor regression in sarcomas is attributable to cellular senescence (38). Thus, the efficacy of radiotherapy could be improved by understanding the mechanisms by which IR induces premature senescence and identifying useful biomarkers for prognosis and diagnosis.

Several laboratories have conducted *in vivo* and *in vitro* proteomic analyses to identify differentially expressed proteins involved in radiation signaling or aging (39–41). However, to our knowledge, biomarkers of IR-induced cellular senescence have not been validated nor determined the roles of these proteins in IR-induced senescence. Here, we identified and validated CD and eEF1 as useful biomarkers. These biomarkers have, for the first time, made it possible to distinguish senescent cells from apoptotic, transiently arrested, or autophagic cells (Figs. 2 and 3). CD was up-regulated and eEF1 was down-regulated in senescent cells induced not only by IR and hydrogen peroxide exposure but also by low doses of the chemotherapeutic drugs. In contrast, CD levels were down-regulated, and eEF1 levels were unchanged under apoptotic conditions. We also observed that CD and eEF1 levels were not changed in response to transient cell cycle arrest, whereas their levels were decreased in autophagic cells. Alterations in CD and eEF1A1 levels were reproducible in replicative or oncogene-induced senescence. However, because eEF1B2 was increased or unchanged in these forms of senescence, it seems to be a less relevant marker than CD and eEF1A1. Together, our findings show that CD and eEF1A1 are promising markers for the detection of cellular senescence. Until now, it has been unclear whether alterations in the levels of identified biomarkers are unique to senescence or are more generally related to cessation of cell proliferation (42). Although p21 and p53 are thought to be the best

established markers of senescence currently available (12), our results show that p21 and p53 are not reliable senescence markers because they show altered protein levels during apoptosis or transient cell cycle arrest. Our results strongly suggest that changes of CD and eEF1 protein levels can accurately predict final cell fates (i.e., cellular senescence, apoptosis, transient cell cycle arrest, or autophagy) following a variety of treatments (Supplementary Table S2).

The eEFs, including eEF1A and eEF1B, are required for the elongation step of translation. The eEFs also have noncanonical functions unrelated to protein synthesis (43). Emerging data show that translation factors participate in the control of cell proliferation, suggesting that these factors may serve as targets for anticancer strategies (44). Our results have led us to surmise that eEF1A1 and eEF1B2 have distinct noncanonical functions in intracellular signaling cascades. That is, eEF1A1 may play a role in senescence pathway, whereas eEF1B2 may contribute to apoptotic pathway. In this study, the decreased level of eEF1 seen during senescence was due to neither a decrease in mRNA nor proteasomal degradation. Because binding of TIAR to eEF1 mRNA regulates eEF1 expression, the eEF1 levels might be regulated by TIAR in senescent cells (45).

CD is a ubiquitous lysosomal aspartic endoproteinase (46). CD is overexpressed in cancer cells, where it enhances cell proliferation, tumorigenesis, and metastasis (47). Several studies suggest that CD participates in the signaling pathways leading to cell death. In addition, CD levels are significantly increased during the normal aging process (48). Here, CD was dramatically increased during senescence and decreased during apoptosis. Taken together, it suggests that regulation of CD expression would be an effective strategy for manipulating senescence and apoptosis pathways.

Tremendous advances have been made in our understanding of senescence during the past half century. Many genes that undergo changes in expression in senescent cells have been identified; however, whether these changes in gene expression contribute to senescence phenotypes or are simply a consequence of senescence is unknown (49). We have shown not only that CD and eEF1 are useful marker molecules for detecting senescent cancer cells but also that these molecules have critical functions in the regulation of cell proliferation. In addition, we show that senescence-associated changes in CD and eEF1 levels can be extended to an irradiated xenografted mouse model. Nevertheless, more extensive studies with experimental animals and patient samples will be required to definitively assess the value of CD and eEF1 as senescence markers *in vivo*.

The factors governing cellular decisions to undergo senescence, apoptosis, or transient growth arrest are incompletely understood. Rapid and complete DNA repair is thought to quickly terminate p53-p21 signaling, whereas slow and incomplete repair results in sustained signaling, ultimately inducing senescence or apoptosis (49). Genome-wide gene expression analysis has revealed that very limited overlap exists among gene expression profiles of cells undergoing senescence in response to different stimuli (41). Understanding these mechanisms will be necessary for developing alternative, less toxic cancer therapies, which aim to induce cellular senescence. In the meantime, eEF1 and CD may serve as valuable biomarkers for cellular senescence induced by IR, anticancer drugs, or other treatments.

Disclosure of Potential Conflicts of Interest

No potential conflicts of interest were disclosed.

Acknowledgments

Received 10/20/08; revised 3/9/09; accepted 3/14/09.

Grant support: National Nuclear Technology Program from The Ministry of Education, Science, and Technology of Korea.

The costs of publication of this article were defrayed in part by the payment of page charges. This article must therefore be hereby marked *advertisement* in accordance with 18 U.S.C. Section 1734 solely to indicate this fact.

References

1. Hayflick L, Moorehead PS. The serial cultivation of human diploid cell strains. Exp Cell Res 1961;25:585–621.
2. Dimri GP, Lee X, Basile G, et al. A biomarker that identifies senescent human cells in culture and in aging skin *in vivo*. Proc Natl Acad Sci U S A 1995;92:9363–7.
3. Chang BD, Xuan Y, Broude EV, et al. Role of p53 and p21waf1/cip1 in senescence-like terminal proliferation arrest induced in human tumor cells by chemotherapeutic drugs. Oncogene 1999;8:4808–18.
4. Serrano M, Lin AW, McCurrach ME, et al. Oncogenic ras provokes premature cell senescence associated with accumulation of p53 and p16INK4a. Cell 1997;88:593–602.
5. Jones KR, Elmore LW, Jackson-Cook C, et al. p53-dependent accelerated senescence induced by ionizing radiation in breast tumour cells. Int J Radiat Biol 2005;81:445–58.
6. Ronninson IB, Broude EV, Chang BD. If not apoptosis, then what? Treatment-induced senescence and mitotic catastrophe in tumor cells. Drug Resist Update 2001;4:303–13.
7. Gewirtz DA, Holt SE, Elmore LW. Accelerated senescence: an emerging role in tumor cell response to chemotherapy and radiation. Biochem Pharmacol 2008;76:947–57.
8. Serrano M. Cancer regression by senescence. N Engl J Med 2007;356:1996–7.
9. Campisi J. Suppressing cancer: the important of being senescent. Science 2005;309:886–7.
10. Collado M, Gil J, Efeyan A, et al. Tumor biology: senescence in premalignant tumors. Nature 2005;436:642.
11. Narita M, Lowe SW. Senescence comes of age. Nat Med 2005;11:920–2.
12. Collado M, Serrano M. The power and the promise of oncogene-induced senescence markers. Nat Rev Cancer 2006;6:472–6.
13. Choi JA, Park MT, Kang CM, et al. Opposite effects of Ha-Ras and Ki-Ras on radiation-induced apoptosis via differential activation of PI3K/Akt and Rac/p38 mitogen-activated protein kinase signaling pathways. Oncogene 2004;23:9–20.
14. Kim KB, Lee JW, Lee CS, Kim BW, Choo HJ, Jung SY, et al. Oxidation-reduction respiratory chains and ATP synthase complex are localized in detergent-resistant lipid rafts. Proteomics 2006;6:2444–53.
15. Lee JS, Huang TQ, Lee JJ, Pack JK, Jang JJ, Seo JS. Subchronic exposure of hsp70.1-deficient mice to radiofrequency radiation. Int J Radiat Biol 2005;81:781–92.
16. Stein GH, Drullinger LF, Soulard A, Duliæ V. Differential roles for cyclin-dependent kinase inhibitors p21 and p16 in the mechanisms of senescence and differentiation in human fibroblasts. Mol Cell Biol 1999;19:2109–17.
17. Cayrol Knibiehler M, Ducommun B. p21 binding to PCNA causes G_1 and G_2 cell cycle arrest in p53-deficient cells. Oncogene 1998;16:311–20.
18. Han Z, Wei W, Dunaway S, et al. Role of p21 in apoptosis and senescence of human colon cancer cells treated with camptothecin. J Biol Chem 2002;277:17154–60.
19. Poele RH, Okorokov AL, Jardine L, Cummings J, Joel SP. DNA damage is able to induce senescence in tumor cells *in vitro* and *in vivo*. Cancer Res 2002;62:1876–83.
20. Chen QM, Bartholomew JC, Campisi J, Acosta M, Reagan JD, Ames BN. Molecular analysis of H_2O_2-induced senescent-like growth arrest in normal human fibroblasts: p53 and Rb control G_1 arrest but not cell replication. Biochem J 1998;332:43–50.
21. Liu J, Li C, Ahlborn TE, Spence MJ, Meng L, Boxer LM. The expression of p53 tumor suppressor gene in breast cancer cells is down-regulated by cytokine oncostatin M. Cell Growth Differ 1999;10:677–83.
22. Chang BD, Broude EV, Dokmanovic M, et al. A senescence-like phenotype distinguishes tumor cells that undergo terminal proliferation arrest after exposure to anticancer agents. Cancer Res 1999;59:3761–7.
23. Eom YW, Kom MA, Park SS, et al. Two distinct modes of cell death induced by doxorubicin: apoptosis and cell death through mitotic catastrophe accompanied by senescence-like phenotype. Oncogene 2005;24:4765–77.
24. Haper JV. Synchronization of cell populations in G_1/S and G_2/M phases of the cell cycle. Methods Mol Biol 2005;296:157–66.
25. Kim EH, Sohn S, Kwon HJ, et al. Sodium selenite induces superoxide-mediated mitochondrial damage and subsequent autophagic cell death in malignant glioma cells. Cancer Res 2007;67:6314–24.

26. Bursch W, Karwan A, Mayer M, et al. Cell death and autophagy: cytokines, drugs, and nutritional factors. Toxicology 2008;254:147–57.

27. Li DD, Wang LL, Deng R, et al. The pivotal role of c-Jun NH_2-terminal kinase-mediated Beclin 1 expression during anticancer agents-induced autophagy in cancer cells. Oncogene 2009;28:886–98.

28. Johansson AC, Steen H, Ollinger K, Roberg K. Cathepsin D mediates cytochrome *c* release and caspase activation in human fibroblast apoptosis induced by staurosporine. Cell Death Differ 2003;10:1253–9.

29. Zhang P, Castedo M, TaoY, et al. Caspase independence of radio-induced cell death. Oncogene 2006;25:7758–70.

30. Bihani T, Chicas A, Lo CP, Lon AW. Dissecting the senescence-like program in tumor cells activated by Ras signaling. J Biol Chem 2007;282:2666–75.

31. Mirzayans R, Scott A, Cameron M, Murray D. Induction of accelerated senescence by γ radiation in human solid tumor-derived cell lines expressing wild-type TP53. Radiat Res 2005;163:53–62.

32. Xue W, Zender L, Miething C, et al. Senescence and tumour clearance is triggered by p53 restoration in murine liver carcinomas. Nature 2007;445:656–60.

33. Sarkisian CJ, Keister BA, Stairs DB, Boxer RB, et al. Dose-dependent oncogene-induced senescence *in vivo* and its evasion during mammary tumorigenesis. Nat Cell Biol 2007;9:493–505.

34. Wu C-H, van Riggelen J, Yetil A, Fan AC, Bachireddy P, Felsher DW. Cellular senescence is an important mechanism of tumor regression upon c-Myc inactivation. Proc Natl Acad Sci U S A 2007;104:13028–33.

35. Chen Z, Trotman LC, Shaffer D, et al. Crucial role of p53-dependent cellular senescence in suppression of Pten-deficient tumorigenesis. Nature 2005;436:725–30.

36. Feldser DM, Greider CW. Short telomeres limit tumor progression *in vivo* by inducing senescence. Cancer Cell 2007;11:461–9.

37. Cosme-Blanco W, Shen MF, Lazar AJ, et al. Telomere dysfunction suppresses spontaneous tumorigenesis *in vivo* by initiating p53-dependent cellular senescence. EMBO Rep 2007;8:497–503.

38. Ventura A, Kirsch DG, McLaughlin ME, et al. Restoration of p53 function leads to tumour regression *in vivo*. Nature 2007;445:661–5.

39. Cho YM, Bae SH, Choi SY, et al. Differential expression of the liver proteome in senescence accelerated mice. Proteomics 2003;3:1883–94.

40. Zhang B, Su YP, Ai GP, et al. Differentially expressed proteins of γ-ray irradiated mouse intestinal epithelial cells by two-dimensional electrophoresis and MALDI-TOF mass spectrometry. Word J Gastroenterol 2003;9:2726–31.

41. Piec I, Listrat A, Alliot J, et al. Differential proteome analysis of aging in rat skeletal muscle. FASEB J 2005;19:1143–5.

42. Zhang H. Molecular signaling and genetic pathway of senescence: its role in tumorigenesis and aging. J Cell Physiol 2007;210:567–74.

43. Lamberti A, Caraglia M, Longo O, et al. The translation elongation factor 1A in tumorigenesis, signal transduction and apoptosis: review article. Amino Acids 2004;26:443–8.

44. Caraglia M, Budillon A, Vitale G, Lupoli G, Tagliaferro P, Abruzzese A. Modulation of molecular mechanisms involved in protein synthesis machinery as a new tool for control of cell proliferation. Eur J Biochem 2000;267:3919–36.

45. Mazan-Mamczarz K, Lal A, Martindale JL, Kawai T, Gorospe M. Translational repression by RNA-binding protein TIAR. Mol Cell Biol 2006;26:2716–27.

46. Barrett AJ. Cathepsin D. purification of isoenzymes from human and chicken liver. Biochem J 1970;117:601–7.

47. Glondu M, Liaudet-Coopman E, Derocq D, Platet N, Rochefort H, Garcia M. Down-regulation of cathepsin-D expression by antisense gene transfer inhibits tumor growth and experimental lung metastasis of human breast cancer cells. Oncogene 2002;21:5127–34.

48. Nakanishi H, Amano T, Sastradipura DF, et al. Increased expression of cathepsin E and D in neurons of the aged rat brain and their colocalization with lipofuscin and carboxy-terminal fragments of Alzheimer amyloid precursor protein. J Neurochem 1997;68:739–49.

49. Campisi J, d'Adda di Fagagna F. Cellular senescence: when bad things happen to good cells. Nat Rev Mol Cell Biol 2007;8:729–40.